

Homogeneity-Based Higher-Order Sliding Mode Controller Design for Permanent Magnet Linear Synchronous Motor

Xi Zhang, Junmin Pan
Department of Electrical Engineering
Shanghai Jiao Tong University
No.800, Dongchuan Road, Shanghai 200030
P. R. China

Abstract:-The permanent magnet linear synchronous motor (PMLSM) is sensitive to various disturbances such as the load disturbances, parameter perturbations, end effect and so on. To overcome this trouble, a new nonlinear robust controller using the homogeneity-based higher-order sliding mode control technique for the PMLSM is proposed. The detailed systematic controller design procedure is discussed. A digital-signal-processor (DSP) –based PMLSM position control system is implemented. The simulation and experimental results under different parameter and load variations are discussed and compared. The proposed control system shows good robustness and high accuracy in spite of the uncertainties, which confirms the theoretical analysis.

Key-Words: PMLSM, homogeneity, higher-order sliding mode, DSP

1 Introduction

Unlike rotary motors, it is not required for linear motors to indirectly couple mechanisms such as gear boxes, chains and screws, which will greatly reduce the effects of contact-types of nonlinearities and disturbances such as backlash and frictional forces [1]. The advantages of the PMLSM include simple mechanical construction, high speed, high acceleration and high motion precision. Therefore, the PMLSM is suitable for high-performance servo applications and has been used widely for the industrial robots, machine tools, semiconductor manufacturing systems, X-Y driving devices and so on [2, 3]. However, the PMLSM is sensitive to the load disturbances and parameter perturbations in the servo drive system because it is not equipped with auxiliary mechanisms such as gears or ball screws. In addition, the end effect makes the thrust force control more difficult [4]. How to compensate these disturbances which directly impose on the mover of the PMLSM and cause unsatisfying dynamic performance is very important in direct drive applications.

Due to the typical precision positioning requirements and low offset tolerance of their applications, the control of the PMLSM under the influence of disturbances is particularly challenging since the conventional PID control usually may not suffice in these application domains [5]. There has been considerable research on applications of advanced control schemes for the PMLSM. A disturbance suppression control system with the force feedforward action to suppress the effect of disturbances was presented in [6]. In such a system,

the disturbances can be detected by the disturbance observer. Feedforward control is used in the force or torque controllers to obtain robustness. However, the inverse dynamic based disturbance observer cannot guarantee sufficient robustness for the servo drive system if the disturbances are large. The linearization method has been successfully used for the PMLSM [7]. This method, however, requires accurate parameters of the PMLSM and complex control procedures. In last few years, some research has focused on applications of the feedforward neural network (NN) for the PMLSM. In [8], an on-line trained fuzzy NN (FNN) controller was proposed to control a permanent magnet synchronous servo motor drive. However, the FNN's application domain is limited to the static problem due to the feedforward network structure, and the weight updates of the feedforward NN do not utilize the internal information of the NN, and the function approximation is sensitive to the training data.

The standard sliding mode control technique in the variable structure control is a very effective nonlinear robust control approach. The basic idea is to force the state via a discontinuous feedback to move on a prescribed manifold [9-11]. However, the specific problem entailed by this technique is the chattering effect which influences the practical applications. This paper focuses on the application of the homogeneity-based higher-order sliding mode control technique for the PMLSM control system. By using this approach, the chattering effect is totally removed, and higher-order precision is provided whereas all the qualities of standard sliding mode are kept. Meanwhile, the homogeneity provides for the

highest possible asymptotic accuracy in the presence of the uncertainties [17]. To the authors' best knowledge, this is the first time that the homogeneity-based higher-order sliding mode control algorithm is applied to the PMLSM position control system. Both the simulation and experimental results show the proposed controller has a good disturbance-rejection performance and tracks different position commands well compared with the conventional three-closed-loop PID controller. Thus, the effectiveness of the proposed system and correctness of the theoretical analysis are testified.

2 Mathematical Model of PMLSM

As shown in Fig.1, the PMLSM studied in this paper is a single-side flat motor which comprises a long stationary "secondary" and a moving short "primary". The secondary is equipped with a sequence of Neodymium-Iron-Boron (NdFeB) permanent-magnet with a guidance rail and linear scale. The primary contains the core armature winding and Hall sensing elements. The electromagnetic thrust force is generated by the interaction between the secondary NdFeB magnet and magnetic field of AC windings in the mover driven by a pulse width modulation (PWM) voltage source inverter. The motion of the PMLSM is highly controllable as the electromagnetic thrust force is directly added to the mechanical system without coupling mechanism.



Fig.1. PMLSM used for study

The d - q dynamic model for the PMLSM is studied. The d - q coordinate system is a "rotating" reference frame that moves at a synchronous speed. The voltage equations of the PMLSM can be described as follows [12]:

$$U_d = Ri_d + \frac{d\lambda_d}{dt} - \frac{\pi}{\tau} n_p v \lambda_q \quad (1)$$

$$U_q = Ri_q + \frac{d\lambda_q}{dt} + \frac{\pi}{\tau} n_p v \lambda_d \quad (2)$$

$$\lambda_d = L_d i_d + \psi \quad (3)$$

$$\lambda_q = L_q i_q \quad (4)$$

where λ_d and λ_q are the direct-axis and quadrature-axis primary flux, respectively; v is the

linear speed of the mover; U_d and U_q are the direct-axis and quadrature-axis primary voltage, respectively; i_d and i_q are the direct-axis and quadrature-axis primary current, respectively; R is the primary winding resistance; L_d and L_q are the direct-axis and quadrature-axis primary inductance, respectively; n_p stands for the number of the pole pairs; ψ and τ are the permanent magnet flux and polar pitch, respectively.

The electromagnetic thrust force is

$$F_e = \frac{P_e}{v} = \frac{3\pi n_p [\psi i_q + (L_d - L_q) i_d i_q]}{2\tau} \quad (5)$$

and the mover dynamic equation is

$$F_e = M \frac{dv}{dt} + Bv + F_l + F_d \quad (6)$$

where P_e is the electromagnetic power; M is the mass of the primary part; B is the viscous damping coefficient; F_l and F_d are the load force and end effect force, respectively.

The machine considered is a surface mounted PMLSM, so the quadrature-axis primary inductance is equivalent to the direct-axis inductance, namely, $L_d = L_q = L$. The number of the pole pairs of the PMLSM is $n_p = 1$. Thus, the dynamics of the PMLSM can be derived from (1)-(6) as follows:

$$\frac{di_d}{dt} = -\frac{R}{L} i_d + \frac{\pi}{\tau} v i_q + \frac{1}{L} U_d \quad (7a)$$

$$\frac{di_q}{dt} = -\frac{R}{L} i_q - \frac{\pi}{\tau} v i_d - \frac{\psi\pi}{\tau L} v + \frac{1}{L} U_q \quad (7b)$$

$$\frac{dv}{dt} = \frac{3\pi\psi}{2\tau M} i_q - \frac{B}{M} v - \frac{1}{M} (F_l + F_d) \quad (7c)$$

For the sake of terseness, we note that $X = (x_1, x_2, x_3, x_4)^T = (i_d, i_q, S, v)^T$, where S is the linear position of the mover. Let u denote the input $u = [u_1 \ u_2]^T = [u_d \ u_q]^T$. The formalization of the parameters is stated as

$$p_1 = -R/L, \quad p_2 = \pi v / \tau, \quad p_3 = 1/L, \quad p_4 = -\psi\pi / \tau L,$$

$$p_5 = 3\pi\psi / 2\tau M, \quad p_6 = -B/M, \quad F_L = F_l + F_d.$$

Then the dynamic equation of the PMLSM can be rewritten as

$$\dot{x}_1 = p_1 x_1 + p_2 x_2 x_4 + p_3 u_1 \quad (8a)$$

$$\dot{x}_2 = p_1 x_2 - p_2 x_1 x_4 + p_4 x_4 + p_3 u_2 \quad (8b)$$

$$\dot{x}_3 = x_4 \quad (8c)$$

$$\dot{x}_4 = p_5 x_2 + p_6 x_4 - F_L / M \quad (8d)$$

The controller is designed to guarantee the robust performance in presence of parameters and load variations. The field-oriented-control is employed, namely, the reference value of the direct-axis primary current $x_{1d} = 0$. The linear

position of the mover must track a reference trajectory x_{3d} .

3 Proposition of Control Strategy for PMLSM

As we all know, the standard sliding mode features are high accuracy and robustness with respect to various internal and external disturbances. It may be implemented only if the relative degree of the constraint is 1, i.e. control has to appear explicitly already in the first total time derivative of the constraint function. Also, high-frequency control switching may cause the so-called chattering effect [13]. Some researchers relate the chattering behavior to the discontinuity of the sign function on the sliding variable. To overcome the problem, they suggest to replace the sign function in a small vicinity of the surface by a smooth approximation, which implies a small deterioration of accuracy and robustness [14, 15]. In recent years, an approach called “high-order sliding mode” has been proposed. Consider a smooth dynamic system with a smooth output function σ , and let the system be closed by some possibly-dynamical discontinuous feedback. Then provided that successive total time derivatives $\sigma, \dot{\sigma}, \dots, \sigma^{(r-1)}$ are continuous functions of the closed-system state-space variables and the set $\sigma = \dot{\sigma} = \dots = \sigma^{(r-1)} = 0$ is non-empty and consists locally of Filippov trajectories, the motion on the set $\sigma = \dot{\sigma} = \dots = \sigma^{(r-1)} = 0$ is called *r-sliding mode* (*rth order sliding mode*). The *rth* derivative $\sigma^{(r)}$ is mostly supposed to be discontinuous or non-existent. Almost all known higher-order sliding mode controllers possess specific homogeneity properties. The corresponding homogeneity of *r*-sliding controllers is called the *rth-order sliding homogeneity* in [16]. The homogeneity makes the convergence proofs of the higher-order sliding mode controllers standard and provides for the highest possible asymptotic accuracy in the presence of the noises, delays and discrete measurements [17].

3.1 Homogeneity-Based Higher-order Sliding Mode Control

Consider a dynamic system of the form

$$\dot{x} = a(x) + b(x)u, \quad y = \sigma(x, t) \quad (9)$$

where $x \in \mathbb{R}^n$ is the state variable; $u \in \mathbb{R}$ is control; $\sigma \in \mathbb{R}$ is a measured output; the smooth functions a, b, σ are assumed unknown.; the dimension n can also be uncertain. The control objective is to make the output σ vanish in finite time and to keep $\sigma \equiv 0$.

The output σ satisfies an equation of the form

$$\sigma^{(r)} = h(x, t) + g(x, t)v, \quad g = \frac{\partial \sigma^{(r)}}{\partial v} \neq 0, \quad h = \sigma^{(r)} \Big|_{v=0} \quad (10)$$

where h and g are unknown smooth functions, and v is the actual control instead of u which is considered as an additional coordinate increasing the dimension of the initial state space to a unit. Suppose that the inequalities

$$0 < K_m \leq g(x, t) \leq K_M, \quad |h(x, t)| \leq C \quad (11)$$

hold for some $K_m, K_M, C > 0$. (10) and (11) imply the differential inclusion

$$\sigma^{(r)} \in [-C, C] + [K_m, K_M]v \quad (12)$$

A bounded feedback control

$$v = \varphi(\sigma, \dot{\sigma}, \dots, \sigma^{(r-1)}) \quad (13)$$

is constructed such that all trajectories of (12), (13) converge in finite time to the origin $\sigma = \dot{\sigma} = \dots = \sigma^{(r-1)} = 0$ of the *r*-sliding phase space. A differential inclusion $\dot{x} \in F(x)$ is further called a *Filippov differential inclusion* if the vector set $F(x)$ is non-empty, closed, convex, locally bounded and upper-semicontinuous [18].

Definition 1. A function $f: \mathbb{R}^n \rightarrow \mathbb{R}$ (respectively, a vector-set field $F(x) \subset \mathbb{R}^n, x \in \mathbb{R}^n$ or a vector field $f: \mathbb{R}^n \rightarrow \mathbb{R}^n$) is called *homogeneous of the degree* $q \in \mathbb{R}$ with the dilation $d_\kappa: (x_1, x_2, \dots, x_n) \mapsto (\kappa^{m_1} x_1, \kappa^{m_2} x_2, \dots, \kappa^{m_n} x_n)$, where m_1, \dots, m_n are some positive numbers (weights), if for any $\kappa > 0$ the identity $f(x) = \kappa^{-q} d_\kappa^{-1} f(d_\kappa x)$ holds (respectively, $F(x) = \kappa^{-q} d_\kappa^{-1} F(d_\kappa x)$, or $f(x) = \kappa^{-q} d_\kappa^{-1} f(d_\kappa x)$). The non-zero homogeneity degree q of a vector field can always be scaled to ± 1 by an appropriate proportional change of the weights m_1, \dots, m_n .

Note that the homogeneity of a vector field $f(x)$ (a vector-set field $F(x)$) can be equivalently be defined as the invariance of the differential equation $\dot{x} \in f(x)$ (differential inclusion $\dot{x} \in F(x)$) with respect to the combined time-coordinate transformation:

$$G_\kappa: (t, x) \mapsto (\kappa^p t, d_\kappa x), \quad p = -q.$$

Property 1. A differential inclusion $\dot{x} \in F(x)$ (equation $\dot{x} = f(x)$) is further called *globally uniformly finite-time stable at 0*, if it is Lyapunov stable and for any $R > 0$ exists $T > 0$, such that any trajectory starting within the disk $\|x\| < R$ stabilizes at zeros in the time T .

Property 2. A differential inclusion $\dot{x} \in F(x)$ (equation $\dot{x} = f(x)$) is further called *globally uniformly asymptotically stable at 0*, if it is Lyapunov stable and for

any $R>0$, $\varepsilon>0$, $T>0$ exists such that any trajectory starting within the disk $\|x\|<R$ enters the disk $\|x\|<\varepsilon$ in the time T to stay there forever. A set D is called retractable if $d_\kappa D \subset D$ for any $\kappa<1$.

Property 3. A homogeneous differential inclusion $\dot{x} \in F(x)$ (equation $\dot{x} = f(x)$) is further called contractive, if there are 2 compact sets D_1, D_2 and $T>0$ such that D_2 lies in the interior of D_1 and contains the origin, D_1 is dilation-retractable, and all trajectories starting at the time 0 within D_1 are localized in D_2 at the time moment T .

Theorem 1. Let $\dot{x} \in F(x)$ be a homogeneous Filippov inclusion with a negative homogeneous degree $-p$. Then properties 1, 2 and 3 are equivalent and the maximal settling time is a continuous homogeneous function of the initial conditions of the degree p .

Corollary 1. The global uniform finite-time stability of homogeneous differential equations (Filippov inclusions) with negative homogeneous degree is robust with respect to homogeneous perturbations causing locally small changes of the equation (inclusion) graph.

Definition 2. Scaling the system homogeneity degree to -1 , achieve that the homogeneity weights of $t, \sigma, \dot{\sigma}, \dots, \sigma^{(r-1)}$ are $1, r, r-1, \dots, 1$, respectively. This homogeneity is further called the r -sliding homogeneity. The inclusion (12), (13) and controller (13) are called r -sliding homogeneous if for any $\kappa>0$ the combined time-coordinate transformation

$$G_\kappa : (t, \sigma, \dot{\sigma}, \dots, \sigma^{(r-1)}) \mapsto (\kappa t, \kappa^r \sigma, \kappa^{r-1} \dot{\sigma}, \dots, \kappa \sigma^{(r-1)}) \quad (14)$$

preserves the closed-loop inclusion (12), (13).

Transformation (14) transfers (12), (13) into

$$\frac{d^r(\kappa^r \sigma)}{(d\kappa t)^r} \in [-C, C] + [K_m, K_M] \varphi(\kappa^r \sigma, \kappa^{r-1} \dot{\sigma}, \dots, \kappa \sigma^{(r-1)}) \quad (15)$$

Hence, (13) is r -sliding homogeneous iff

$$\varphi(\kappa^r \sigma, \kappa^{r-1} \dot{\sigma}, \dots, \kappa \sigma^{(r-1)}) \equiv \varphi(\sigma, \dot{\sigma}, \dots, \sigma^{(r-1)}) \quad (16)$$

Such a homogeneous controller is inevitably discontinuous at the origin $(0, \dots, 0)$, unless φ is a constant function. It is also uniformly bounded, since it is locally bounded and takes on all its values in any vicinity of the origin.

Let q be the least common multiple of $1, 2, \dots, r$, and $\beta_1, \dots, \beta_{r-1} > 0$. Define

$$N_{i,r} = \left(|\sigma|^{q/r} + |\dot{\sigma}|^{q/(r-1)} + \dots + |\sigma^{(i-1)}|^{q/(r-i+1)} \right)^{(r-i)/q} \quad (17)$$

$$\varphi_{0,r} = \text{sign } \sigma, \quad \varphi_{i,r} = \text{sign}(\sigma^{(i)} + \beta_i N_{i,r} \varphi_{i-1,r}) \quad (18)$$

$i = 1, \dots, r-1$

Then $v = -\alpha \varphi_{r-1,r}(\sigma, \dot{\sigma}, \dots, \sigma^{(r-1)})$ defines the standard r -sliding controller [16]. The main drawback of the controller is some trajectory chattering during the transient caused by the complicated structure of the control discontinuity set. The output-feedback performance with noisy measurements is also problematic. Corollary 1 allows new controller structures to be produced transforming known homogeneous controllers. Define the homogeneous norm and the saturation function [17]

$$N_r = N_{r,r} = (|\sigma|^{q/r} + |\dot{\sigma}|^{q/(r-1)} + \dots + |\sigma^{(r-1)}|^{q/(r-1)})^{1/q} \quad (19)$$

$$\text{sat}(z, \varepsilon) = \min[1, \max(-1, z/\varepsilon)] \quad (20)$$

Let $i = 1, \dots, r-1$. The construction is as follows:

$$\phi_{0,r} = \text{sign } \sigma, \quad \phi_{i,r} = \text{sat}\left[\frac{\sigma^{(i)} + \beta_i N_{i,r} \varphi_{i-1,r}}{N_r^{r-i}}, \varepsilon_i\right] \quad (21)$$

Obviously $\phi_{i,r}$ is homogeneous of the weight 0 and continuous everywhere except

$\sigma = \dot{\sigma} = \dots = \sigma^{(r-1)} = 0$. The controller

$$v = -\alpha \phi_{r-1,r}(\sigma, \dot{\sigma}, \dots, \sigma^{(r-1)}) \quad (22)$$

ensures the finite-time convergence to the r -sliding mode $\sigma \equiv 0$ with properly chosen α, β_i and small ε_i . It can be shown that β_i and ε_i can be chosen once for each r , and only $\alpha > 0$ is to be adjusted with respect to C, K_m, K_M .

3.2 Design of the Homogeneity-Based Second-Order Sliding Mode Controller for PMLSM

The content in this section is to design a MIMO homogeneity-based second-order sliding mode controller for the PMLSM. The aim is to force the direct-axis current x_1 and linear position x_3 to be the reference values x_{1d} and x_{3d} , respectively. Take

$$\sigma_1 = x_1 - x_{1d} = e_1 \quad (23)$$

Note that the relative degree of σ_1 equals 1. Let $e_3 = x_3 - x_{3d}$, and

$$\sigma_2 = \ddot{e}_3 + \lambda_1 \dot{e}_3 + \lambda_2 e_3 \quad (24)$$

where λ_1 and λ_2 are positive constant numbers such that $H(z) = \ddot{z} + \lambda_1 \dot{z} + \lambda_2 z$ is Hurwitz polynomial. The relative degree of σ_2 is also 1. Based on (8), the first and second time derivatives of σ_1 can be achieved as follows

$$\dot{\sigma}_1 = \dot{e}_1 = p_1 x_1 + p_2 x_2 x_4 + p_3 u_1 - \dot{x}_{1d} \quad (25)$$

$$\begin{aligned} \ddot{\sigma}_1 &= p_1 \dot{x}_1 + p_2 \dot{x}_2 x_4 + p_2 x_2 \dot{x}_4 - \ddot{x}_{1d} + p_3 \dot{u}_1 \\ &= p_1 (p_1 x_1 + p_2 x_2 x_4 + p_3 u_1) \\ &\quad + p_2 x_4 (p_1 x_2 - p_2 x_1 x_4 + p_4 x_4 + p_3 u_2) \end{aligned}$$

$$\begin{aligned} &+ p_2 x_2 (p_5 x_2 + p_6 x_4 - F_L / M) - \ddot{x}_{1d} + p_3 \dot{u}_1 \\ &= C_1(x) + D_1(x) \dot{u}_1 \end{aligned} \quad (26)$$

The first and second time derivatives of σ_1 can also be obtained as follows

$$\begin{aligned} \dot{\sigma}_2 &= p_5 (p_1 x_2 - p_2 x_1 x_4 + p_4 x_4 + p_3 u_2) \\ &+ (\lambda_1 + p_6) (p_5 x_2 + p_6 x_4 - F_L / M) \\ &- \dot{F}_L / M + \lambda_2 x_4 - x_{3d}^{(3)} - \lambda_1 \ddot{x}_{3d} - \lambda_2 \dot{x}_{3d} \end{aligned} \quad (27)$$

$$\begin{aligned} \ddot{\sigma}_2 &= -x_{3d}^{(4)} - \lambda_1 x_{3d}^{(3)} - \lambda_2 \ddot{x}_{3d} + (p_1 p_5 + \lambda_1 p_5 \\ &+ p_1 p_5) (p_1 x_2 - p_2 x_1 x_4 + p_4 x_4 + p_3 u_2) \\ &+ (\lambda_1 p_6 + p_6^2 + p_5 x_4 + \lambda_2) (p_5 x_2 + p_6 x_4 - F_L / M) \\ &- p_2 p_5 (\dot{x}_1 x_4 + x_1 \dot{x}_4) - (\lambda_1 + p_6) \dot{F}_L / M - \ddot{F}_L / M + p_3 \dot{u}_2 \\ &= C_2(x) + D_2(x) \dot{u}_2 \end{aligned} \quad (28)$$

The generalized load force F_L is considered as a perturbation. Because the electromagnetic time constant is much smaller than the mechanical time constant, the variation of the generalized load force F_L is very slow compared with electrical variations. F_L is supposed to be bounded as well as its two first time derivatives. C_{1N} , C_{2N} , and $D_{1N} = D_{2N} = p_{3N} = d_N$ are the known nominal expressions by substituting the system nominal parameters into $C_1(x)$, $C_2(x)$, $D_1(x)$ and $D_2(x)$.

Let

$$\ddot{\sigma} = C(x) + D(x) [\dot{u}_1 \quad \dot{u}_2]^T \quad (29)$$

where

$$\begin{aligned} C(x) &= \begin{pmatrix} C_1(x) \\ C_2(x) \end{pmatrix} = \begin{pmatrix} C_{1N} \\ C_{2N} \end{pmatrix} + \begin{pmatrix} \Delta C_1 \\ \Delta C_2 \end{pmatrix} = C_N + \Delta C, \\ D(x) &= \begin{pmatrix} D_1(x) & 0 \\ 0 & D_2(x) \end{pmatrix} = \begin{pmatrix} d_N & 0 \\ 0 & d_N \end{pmatrix} + \begin{pmatrix} \Delta d & 0 \\ 0 & \Delta d \end{pmatrix} \\ &= D_N + \Delta D \end{aligned} \quad (30)$$

ΔC and ΔD contain all the uncertainties due to parameters and load force variations. Since $p_{3N} \neq 0$, the diagonal matrix D_N is reversible. However, the model (29) is uncertain. The conception of a feedback linearization technique is employed:

$$[\dot{u}_1 \quad \dot{u}_2]^T = D_N^{-1} [-C_N + [v_1 \quad v_2]^T] \quad (31)$$

The actual input $v = [v_1 \quad v_2]^T$ is designed to stabilize the new system. Substitute (31) into (29), a new expression can be achieved

$$\begin{bmatrix} \ddot{\sigma}_1 \\ \ddot{\sigma}_2 \end{bmatrix} = \begin{bmatrix} \hat{C}_1 \\ \hat{C}_2 \end{bmatrix} + \begin{pmatrix} \hat{D}_1 & 0 \\ 0 & \hat{D}_2 \end{pmatrix} \begin{bmatrix} v_1 \\ v_2 \end{bmatrix} \quad (32)$$

where

$$\hat{C}_1 = \Delta C_1 - \frac{\Delta d C_{1N}}{d_N} \quad \hat{C}_2 = \Delta C_2 - \frac{\Delta d C_{2N}}{d_N}$$

$$\hat{D}_1 = \hat{D}_2 = 1 + \frac{\Delta d}{d_N} \quad (33)$$

Thus, the MIMO problem is decoupled into a set of single-input problems which satisfy the requirements of homogeneity-based higher-order sliding mode control technique. Since the state variables and the perturbations of parameters are bounded, and under the assumption that $|\Delta d| < |D_1| = |D_2|$, there exist positive constant numbers M_1 , M_2 , K_m and K_M so that

$$|\hat{C}_1| < M_1 \quad |\hat{C}_2| < M_2 \quad 0 < K_m < \hat{D}_1 = \hat{D}_2 < K_M \quad (34)$$

which is equivalent to (11).

The homogeneity approach to higher-order sliding mode design in the previous section is used to design the robust controller for PMLSM. Achieve $r = 2$, $q = 2$ and let $\varepsilon_1 = 0.2$, thus,

$$N_2 = N_{2,2} = (|\sigma|^2 + |\dot{\sigma}|)^{1/2} \quad (35)$$

$$\phi_{0,2} = \text{sign } \sigma,$$

$$\phi_{1,2} = \text{sat}[(\dot{\sigma} + |\sigma|^{1/2} \text{sign } \sigma) / (|\dot{\sigma}|^2 + |\sigma|)^{1/2}, 0.2] \quad (36)$$

According to (22), the homogeneity-based 2-sliding mode controller is designed as

$$v_j = -\alpha_j \text{sat}[(\dot{\sigma}_j + |\sigma_j|^{1/2} \text{sign } \sigma_j) / (|\dot{\sigma}_j|^2 + |\sigma_j|)^{1/2}, 0.2], \quad j = 1, 2 \quad (37)$$

where $\alpha_j, j = 1, 2$ is a chosen positive constant.

3.3 Design of the Force Observer

Since the generalized load force F_L is unknown, it can be replaced by its estimated value in (31). Because the variation of F_L is very slow compared with electrical variations, F_L can be considered as a constant in a small time range. F_L and the linear speed v are chosen as new state variables. From (7), it can be obtained as

$$\frac{d\xi}{dt} = H\xi + Aw \quad (38)$$

where

$$\xi = (F_L \quad v)^T, \quad H = \begin{pmatrix} 0 & 0 \\ -\frac{1}{M} & -\frac{B}{M} \end{pmatrix} = \begin{pmatrix} 0 & 0 \\ c_r & a_r \end{pmatrix},$$

$$A = \begin{pmatrix} 0 \\ \frac{3\pi\psi}{2\tau M} \end{pmatrix} = \begin{pmatrix} 0 \\ b_r \end{pmatrix}, \quad w = i_q$$

Obviously, this system can be observed. The observer can be designed as follows:

$$\frac{d\hat{\xi}}{dt} = H\hat{\xi} + Aw + Q(v - E\hat{\xi}) \quad (39)$$

where $P = (q_1 \quad q_2)^T$ is a constant vector, and

$E = (0 \ 1)$. The nominal system parameters are used in (39). From (39), the estimated value F_{LN} of the generalized load force F_L can be obtained. The two first time derivatives of F_{LN} are considered as zero. The construction of the load force observer is shown in Fig. 2.

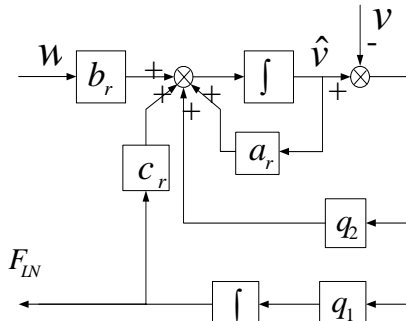


Fig.2. Construction of the force observer

It should be noted that the quadrature-axis primary current can be made not to exceed its maximum permissible value in the PMLSM servo system by employing an asymptotic reference model of the position command. The proposed control system is shown in Fig.3.

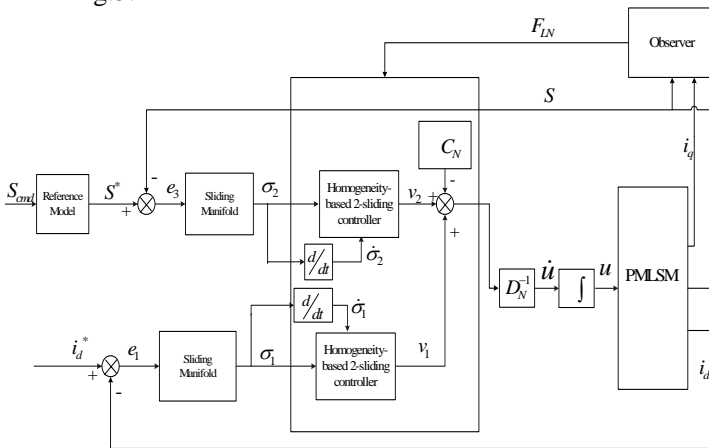


Fig.3. Diagram of the proposed system

4 Simulation and Experimentation

4.1 Simulation

The simulated results can be obtained by the MATLAB package. Tab.1 shows the simulation system parameters which are from the single-side flat PMLSM shown in Fig.1. The stroke length is 800mm. The maximum value of the quadrature-axis current permitted is 15A. To investigate the effectiveness of the proposed sliding mode control system, three simulation cases including a parameter variation and load disturbance are considered here. The PMLSM is in the condition of nominal system parameters without load at Case 1. At Case 2, the mass of mover is increased at $M = 3M_n$ without load. At Case 3, with nominal system parameters, a sudden load of 5.4kg is added at $t=0.4s$. The simulation

results using the proposed scheme are compared with those using the field-oriented-control based three-closed-loop PID servo system of the PMLSM introduced in [12]. By applying the partial model matching method, the PID controller parameters can be solved as follows, the current loop proportional gain is $K_{pC} = 4.5$, the speed loop PID gains are $K_I = 25.9$, $K_p = 2.3$ and $K_D = 0.1$, the position loop proportional gain is $K_{pP} = 19.2$. For the proposed 2-sliding controller, controller parameters are selected as $\lambda_1 = 3100$, $\lambda_2 = 200$, $\alpha_1 = 61000$, $\alpha_2 = 78000$, $q_1 = -1054$ and $q_2 = 75.6$. Moreover, a second-order transfer function of the following form with the rise time of 0.06s is chosen as the reference model for a step command change: $H(s) = \frac{6400}{s^2 + 180s + 6400}$, where s

is the Laplace operator. The reference value of the direct-axis current is set as zero.

TABLE I SYSTEM PARAMETERS OF PMLSM

Primary Winding Resistance	1.23 Ω
Direct-Axis Primary Inductance	8.41mH
Quadrature-Axis Primary Inductance	8.41mH
Permanent Magnet Flux	0.55Wb
Mass of the Primary Part	10.6kg
Polar Pitch	30mm
Viscous Damping Coefficient	2Ns/m

In the simulation, a position step command with the 8mm-amplitude is given. The position responses and quadrature-axis current at three cases using the PID controller and homogeneity-based 2-sliding controller are shown in Fig.4 and Fig.5. As the parameters of the PID controller depend only on the nominal parameters of the drive system, the performance of the servo drive system is sensitive to the parameter variations and load disturbance in the system. As shown in Fig.4, the position tracking response of the square command can be satisfying by using a PID controller only at Case 1. At Case2, the position overshoot phenomenon appears as shown in Fig.4(c) if there is a large parameter variation. When a sudden load is added at Case 3, the error between the position command and actual position is large as shown in Fig.4(e), and the tracking performance is unsatisfying. The position tracking responses using the proposed sliding mode controller at three cases are all satisfying as shown in Figs.5(a), (c) and (e). The robustness using the proposed controller is obvious compared with the PID controller. Meanwhile, it can be observed from the simulated results in Figs.4(b), (d) and (f) that there is no chattering in the quadrature-axis current by employing the homogeneity-based higher-order sliding mode control technique.

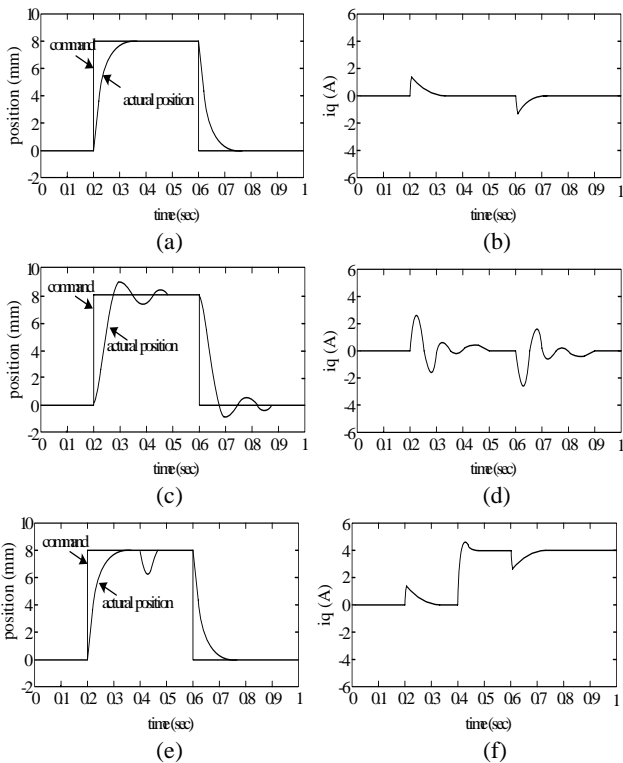


Fig.4. Simulated results using the PID controller (a) position response at Case1 (b) quadrature-axis current at Case 1 (c) position response at Case 2 (d) quadrature-axis current at Case 2 (e) position response at Case3 (f) quadrature-axis current at Case3

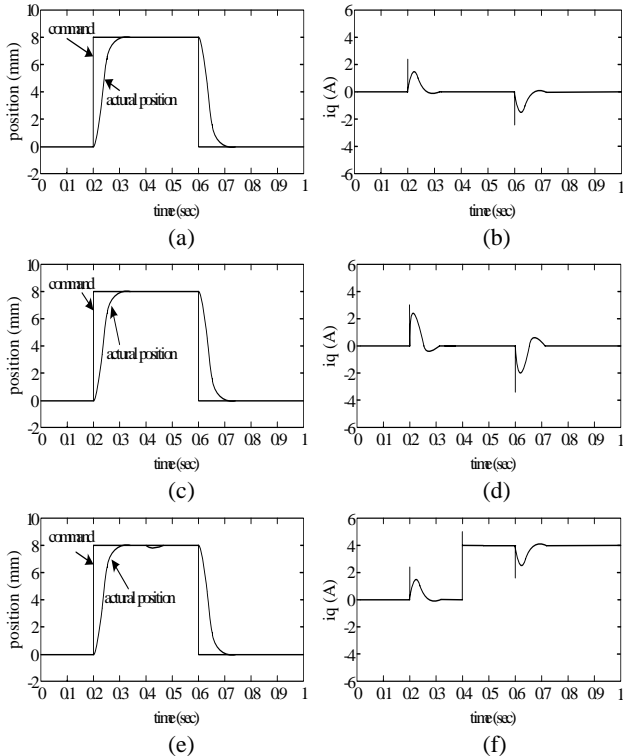


Fig.5. Simulated results using the proposed sliding mode controller (a) position response at Case 1 (b) quadrature-axis current at Case 1 (c) position response at Case 2 (d) quadrature-axis current at Case 2 (e) position response at Case3 (f) quadrature-axis current at Case3

4.2 Experimentation

In the experimental studies, a 32-bit fixed-point microprocessor TMS320F2812 manufactured by Texas Instruments is used which has the advantages of high

speed (150MIPS), 2 sets (4 channels) of QEP inputs, 2 sets (12 channels) of PWM outputs and 12 channels of 12-bit A/D converters (200ns conversion time). The C language is used for the control program. The DC link voltage value is 190V. The inverter legs are made of six insulated gate bipolar transistors (IGBTs). The PWM is implemented with a space-vector modulation technique with the switching frequency of 20kHz. The sampling frequencies of the phase current and position are 10kHz and 5kHz, respectively. A Heidenhaim optical encoder with the resolution of $0.5 \mu\text{m}$ is equipped in the system as a position sensor. The block diagram of the hardware system is shown in Fig.6.

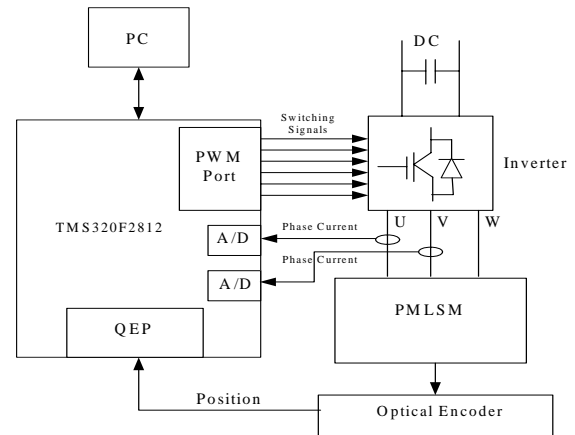


Fig.6. Block diagram of the hardware system

As mentioned above, a sudden load is added at about $t=0.4\text{s}$ at Case 3 in the simulation. However, the accurate moment when load is added is difficult to be decided as delay exists in the practical operation. In the experimentation, a new case of Case 4 is considered. At this case, a load of 5.4kg is added at about $t=2\text{s}$, and a position step command is given at $t=1.7\text{s}$. A position step command with the 8mm-amplitude is given. The experimental results of the two controllers at Case 1, 2 and 4 under the step commands are shown in Fig.7 and Fig.8. Though the experimental results are similar to the simulated results, the minor difference between them is caused by the uncertainties of the real plant. As shown in Figs.7(a), (c) and (e), the dynamic performance of the PID servo drive system is sensitive to the parameter variation and load disturbance. Only the position tracking response of the square command can be satisfying at Case 1. The improvement of the tracking responses at three cases using the proposed sliding mode controller is obvious as shown in Figs.8(a), (c) and (e). It can also be observed from the experimental results in Figs.8(b), (d) and (f) that there is no control chattering in the quadrature-axis current by employing the homogeneity-based higher-order sliding mode control technique. In order to further testify the accuracy of the proposed controller, the position sinusoidal response at Case 2 is considered. The reference sinusoidal position with the 10mm-amplitude is shown in Fig.9(a). It can be viewed in Fig.9(b) that the linear position tracking error does

not exceed $12 \mu\text{m}$, which can completely satisfy the experimental requirements. Fig.9(d) displays the direct-axis current i_d which converges to zero. It can also be seen from Fig.9(c) that chattering of the quadrature-axis current is removed by using the proposed controller.

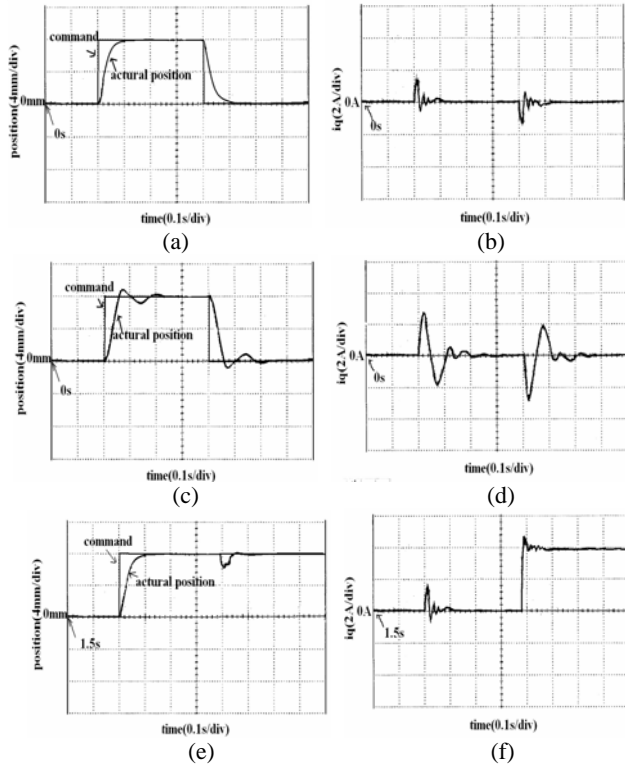


Fig.7. Experimental results using the PID controller under the step response (a) position response at Case1 (b) quadrature-axis current at Case 1 (c) position response at Case 2 (d) quadrature-axis current at Case 2 (e) position response at Case 4 (f) quadrature-axis current at Case 4

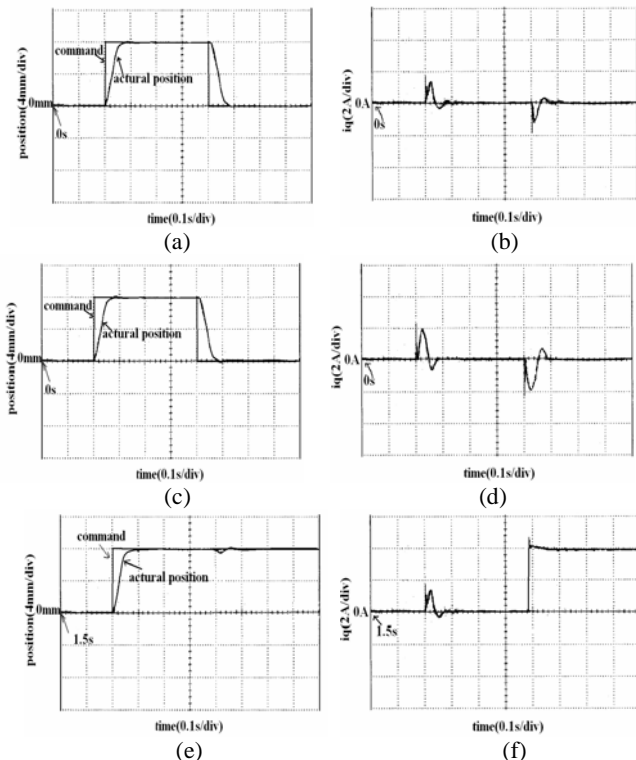


Fig.8. Experimental results using the proposed controller under the step response (a) position response at Case1 (b) quadrature-axis

current at Case 1 (c) position response at Case 2 (d) quadrature-axis current at Case 2 (e) position response at Case 4 (f) quadrature-axis current at Case 4

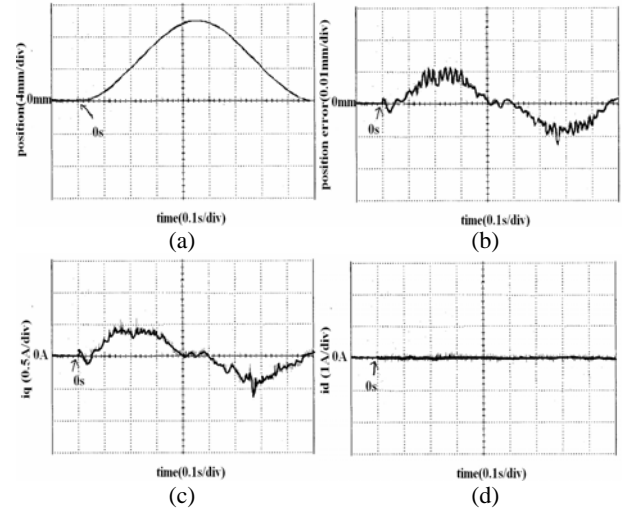


Fig.9. Experimental results of the position sinusoidal response using the proposed controller (a) linear position reference (b) position tracking error (c) quadrature-axis current (d) direct-axis current

5 Conclusion

In this paper, the homogeneity-based higher-order sliding mode control technique is applied to the PMLSM control system. The systematic design methodology of the homogeneity-based 2-sliding controller is discussed. The proposed PMLSM position control system shows the satisfactory tracking performance of excellent robustness in spite of the uncertainties under different position commands. Therefore, the validity of the proposed control system is confirmed.

References:

- [1] S. W. Tam and N. C. Cheung, "An all-digital high performance drive system for linear permanent-magnet synchronous motor," *4th Chinese Power Supplies Society Annual General Meeting*, Beijing, China, 2001, pp. 24-27.
- [2] M. S. Kwak and S. K. Sul, "A new method of partial excitation for dual moving magnet linear synchronous motor," *IEEE Trans. Industry Applications*, vol. 40, no. 2, 2004, pp. 499-505.
- [3] R. D. Thomson, T. Clark and B. Perreault, "Linear synchronous motor propulsion of small transit vehicles," *Proceedings of the 2004 ASME/IEEE Joint Rail Conference*, vol. 27, 2004, pp. 101-107.
- [4] C. E. Miller, A. W. Van Zyl and C. F. Landy, "Modeling a permanent magnet linear synchronous motor for control purposes," *IEEE AFRICON Conference*, vol. 2, 2002, pp. 671-674.
- [5] F. J. Lin, K. K. Shyu and C. H. Lin, "Incremental motion control of linear synchronous motor," *IEEE Trans. Aerospace and Electronic Systems*,

- vol. 38, no. 3, 2002, pp. 1011-1022.
- [6] Z. Z. Liu, F. L. Luo and M. H. Rashid, "Robust high speed and high precision linear motor direct-drive XY-table motion system," *IEE Proceedings: Control Theory and Applications*, vol. 151, no. 2, 2004, pp. 166-173.
- [7] P. Famouri, "Control of a linear permanent magnet brushless dc motor via exact linearization methods," *IEEE Transactions on Energy Conversion*, vol. 7, no. 3, 1992, pp. 544-551.
- [8] F. J. Lin and P. H. Shen, "DSP-based permanent magnet linear synchronous motor servo drive using adaptive fuzzy-neural-network control," *2004 IEEE Conference on Robotics, Automation and Mechatronics*, vol. 1, 2004, pp. 601-606.
- [9] A. Isidori, *Nonlinear Control Systems*, Berlin, New York : Springer-Verlag, 1995
- [10] K. C. Li, T. P. Leung and Y. M. Hu, "Sliding mode control of distributed parameter systems," *Automatica*, vol. 30, no. 12, 1994, pp. 1961-1966.
- [11] J. C. Lo and Y. H. Kuo, "Decoupled fuzzy sliding-mode control," *IEEE Trans. Fuzzy Systems*, vol. 6, no. 3, 1998, pp. 426-435.
- [12] J. F. Gieras and Z. J. Piech, *Linear Synchronous Motors-- Transportation and Automation Systems*, CRC Press, 2000
- [13] L. Fridman, "An averaging approach to chattering," *IEEE Trans. Automatic Control*, vol. 46, no. 8, 2001, pp. 1260-1265.
- [14] V. J. Utkin, *Sliding mode in control and optimization*, Springer-Verlag, Berlin, 1992
- [15] P. Kachroo and M. Tomizuka, "Chattering reduction and error convergence in the sliding-mode control of a class of nonlinear systems," *IEEE Trans. Automatic Control*, vol. 41, no. 7, 1996, pp. 1063-1068.
- [16] A. Levant, "Higher-order sliding modes, differentiation and output-feedback control," *International Journal of Control*, vol. 76, no. 9, 2003, pp. 924-941.
- [17] A. Levant, "Homogeneity approach to high-order sliding mode design," *Automatica*, vol. 41, no. 5, 2005, pp. 823-830.
- [18] A. F. Filippov, *Differential equations with discontinuous right-hand side*, Dordrecht, The Netherlands: Kluwer, 1988